Journal of Biological Physics **30:** 285–303, 2004.

Homogenization of Heterogeneously Coupled Bistable ODE's—Applied to Excitation Waves in Pancreatic Islets of Langerhans

MORTEN GRAM PEDERSEN
Informatics and Mathematical Modelling, The Technical University of Denmark, DK-2800 Lyngby, Denmark
(e-mail: mgp@imm.dtu.dk)

Abstract. We consider a lattice of coupled identical differential equations. The coupling is between nearest neighbors and of resistance type, but the strength of coupling varies from site to site. Such a lattice can, for example, model an islet of Langerhans, where the sites in the lattice model individual but identical β-cells, and the coupling between cells is made of gap junctions.

By using a homogenization technique we approximate the coupled discrete equations by a PDE, basically a nonlinear heat equation (a Fisher equation). For appropriate parameters this equation is known to have wave-solutions. Of importance is the fact, that the resulting diffusion coefficient does not only depend on the average of the coupling, but also on the variance of the strength. This means that the heterogeneity of the coupling strength influences the wave velocity—the greater the variance, the slower is the wave. This result is illustrated by simulations, both of a simple prototype equation, and for a full model of coupled beta-cells in both one and two dimensions, and implies that the natural heterogeneity in the islets of Langerhans should be taken into account.

Key words: homogenization, calcium waves, excitation waves, propagation speed, coupled pancreatic β-cells, gap-junctions

1. Introduction

The pancreatic islets of Langerhans consist of thousands of coupled cells, among these the β-cells produce insulin. To have a proper functioning and insulin production, it is very important that the β-cells co-operate in a synchronized manner, and the coupling between cells made up of gap junctions seems to be crucial for this synchronization ([3, 5] and references herein). In [1] it was shown experimentally that calcium waves could provide a way to synchronize the cells. Using a mathematical model of the β-cells the authors showed that the gap junctions indeed could result in waves of the observed kind. However, the simulated speed was significantly faster (about 200 μm/s) than the experimentally observed speeds (30–100 μm/s), if standard values were used in the model. The authors gave possible

explanations for this speed difference, all involving modifying parameter values.

It was assumed in [1] that the coupling strength was constant from site to site. This is known not to be the case, indeed there is a natural variance of the coupling strengths [7, 5].

We show here that if the authors of [1] had taken into account the natural variance of the coupling strengths of the gap-junctions, they would have seen significantly lower wave-speeds—in some cases—even in the experimentally observed region.

To understand why the average (the arithmetic mean) of the coupling strength is not enough to estimate the propagation speed of the waves, we need the mathematical discipline *homogenization* theory (see [2]), which shows that, it is the *harmonic mean* that determines the velocity—and this will explain why the variance is important.

The paper is organized as follows. In the next section we look at the general case, and see that the homogenization theory can indeed be applied, and the harmonic mean determines the wave speed. This is then used for the Fisher equation (Section 3) to see that the theory estimates the simulated wave-speed very well. We then move on to compare it with the β-cell model, obtaining the results mentioned above. Finally, two-dimensional simulations show that similar conclusions can be made in both the case of the Fisher equations and the β-cell model in 2D. We discuss the results in Section 6. A detailed description of the β-cell model is given in the Appendix.

2. The Model and Homogenization—The Continuum Limit

We consider an finite line of cells modeled by ($j = 0, \ldots, N$)

$$\frac{dv_j}{dt} = f(v_j) + g_{j+1} \cdot (v_{j+1} - v_j) + g_j \cdot (v_{j-1} - v_j). \tag{1}$$

The relevance for β-cells is similar for Eqs. (5) and (6) in [1]. This is discussed further in Section 4.

The distance between neighbors is set to be ϵ such that $v_j = v(j\epsilon)$, and we observe the behavior when $\epsilon \to 0$. Let us first consider the simple case of equal connections, where every $g_i = g = \epsilon^{-2}D$ for a constant D (see also [1]). With $x = j\epsilon$, we get

$$\frac{\partial v}{\partial t}(x) = f(v(x)) + g \cdot (v(x+\epsilon) + v(x-\epsilon) - 2v(x)),$$

or, using a Taylor approximation and letting $\epsilon \to 0$,

$$\frac{\partial v}{\partial t}(x) = f(v) + D\frac{\partial^2 v}{\partial x^2}, \tag{2}$$

which is known to have wave solutions for appropriate f, with propagation velocity proportional to $\sqrt{D}$ [1].

Now, we assume that the connection varies from site to site as described by (1). Let κ_ϵ be a family of differentiable functions with $||\kappa_\epsilon||_\infty$ independent of ϵ. With $g_j = g(j\epsilon) = \epsilon^{-2}\kappa_\epsilon(x)$, $x = j\epsilon$ we get as above:

$$\begin{aligned}\frac{\partial v}{\partial t} &= f(v) + \left(g + \epsilon\frac{\partial g}{\partial x} + o(1)\right)\left(\epsilon\frac{\partial v}{\partial x} + \frac{\epsilon^2}{2}\frac{\partial^2 v}{\partial x^2} + o(\epsilon^3)\right) \\ &\quad + g\cdot\left(-\epsilon\frac{\partial v}{\partial x} + \frac{\epsilon^2}{2}\frac{\partial^2 v}{\partial x^2} + o(\epsilon^3)\right) \\ &= f(v) + \kappa_\epsilon(x)\frac{\partial^2 v}{\partial x^2} + \frac{\partial \kappa_\epsilon}{\partial x}\frac{\partial v}{\partial x} + o(\epsilon) \\ &= f(v) + \frac{\partial}{\partial x}\left(\kappa_\epsilon(x)\frac{\partial v}{\partial x}\right) + o(\epsilon).\end{aligned} \tag{3}$$

2.1. Periodic coupling

We hold the total length constant, $N\epsilon = L$, and assume that the coupling strength is periodic, $g_j = g_{j+J}$ for some J. This can be incorporated in (3) without any loss of generality by assuming that $\kappa_\epsilon(x) = \kappa(\frac{x}{\epsilon})$, where κ is a periodic function of period 1 with $0 < \kappa_1 \le \kappa \le \kappa_2$ for constants κ_1, κ_2. Then we obtain

$$\frac{\partial v}{\partial t} = f(v) + \frac{\partial}{\partial x}\left(\kappa\left(\frac{x}{\epsilon}\right)\frac{\partial v}{\partial x}\right) + o(\epsilon). \tag{4}$$

The theory of such equations in the limit $\epsilon \to 0$ is understood well from material science modeling of a periodic structure and is rigorously covered by the mathematical discipline of *homogenization theory* (see [2]).

In the limit $\epsilon \to 0$ we get the equation [2]:

$$\frac{\partial v}{\partial t} = f(v) + \kappa^*\frac{\partial^2 v}{\partial x} \tag{5}$$

where κ^* *is not* the average of κ, $E(\kappa)$, as one might expect from a first guess, but instead is the *harmonic mean*

$$\kappa^* = \left(E(1/\kappa)\right)^{-1}. \tag{6}$$

We expect that the solution to the discrete Eq. (1) behaves similar to the solution of Eq. (5). Of course, if $\kappa(x) = D$ is constant, we obtain Eq. (2) again.

To understand the implications for the heterogenous case, we consider the simplest case, where

$$\kappa(x) = \begin{cases} g_1 & \text{for } 0 \le x \le 0.5, \\ g_2 & \text{for } 0.5 \le x < 1, \end{cases} \tag{7}$$

$g_2 > g_1$, modeling interchangingly strong and weak coupling.[1] The unique part is that it is not the average $E(g) = \frac{g_1+g_2}{2}$ that determines the wave velocity, but instead

$$\left(\frac{g_1^{-1} + g_2^{-1}}{2}\right)^{-1} = 2 \cdot \frac{g_1 g_2}{g_1 + g_2} = \frac{(E(g) - \sigma(g))(E(g) + \sigma(g))}{E(g)} = E(g) - \frac{\sigma(g)^2}{E(g)},$$

where $\sigma(g) = \frac{g_2-g_1}{2}$ is related to a kind of "standard deviation" of g, i.e., the degree of heterogeneity of the couplings.

In general, we have

$$\kappa^* = (E(1/\kappa))^{-1} \le E(\kappa),$$

and we expect that in the case of wave propagation, a greater variance will lead to slower waves.

2.2. Randomly distributed connections

In the proof of the above [2] the periodicity of κ is not explicitly used—only that

$$\frac{1}{\kappa_\epsilon} \to E(1/\kappa) \text{ weak star in } L_\infty.$$

This should also be true if we choose the connections g_j randomly from a fixed distribution F, i.e., as data coming from a stochastic variable X with distribution F. For sufficiently multiple connections (i.e., ϵ small enough) integrating $\frac{1}{\kappa_\epsilon}$ should be near the average of, not the original distribution, but $E(1/X)$. This would be a consequence of the Law of Large Numbers for weighted averages. Hence, the theory should also work in this case.

3. Numerical Simulations of a Simple Model

3.1. Periodic coupling

We consider a line of 500 cells connected with interchangingly weak and strong connections as indicated in Eq. (7), and with a no-flux boundary condition

($v_0 = v_1, v_{501} = v_{500}$). We observe that the propagation velocity, c, should not depend on the average of the connections, $E(g)$, but instead, we have

$$c_{\text{th}} = K \cdot \sqrt{(E(1/\kappa))^{-1}} = K \cdot \sqrt{E(g) - \frac{\sigma^2}{E(g)}}, \tag{8}$$

where K is a constant, which we can find from the homogeneous case, $\sigma = 0$.

We choose a simple model, the *Fisher equation*, with

$$f(v) = -v(v - a)(v - 1).$$

It is well known [8] that the wave speed in the homogeneous case $\sigma = 0$ is

$$c_{\text{th}}^0 = \sqrt{\frac{D}{2}}(1 - 2a) = \sqrt{\frac{E(g)}{2}}(1 - 2a), \tag{9}$$

so that

$$c_{\text{th}} = \frac{1 - 2a}{\sqrt{2}} \sqrt{E(g) - \frac{\sigma^2}{E(g)}}. \tag{10}$$

We hold $a = 0.1$, $E(g) = 2$ is fixed and σ varies from 0 to 1.9. The initial conditions are $v_j = 0$ for all j. We start a wave by instantaneously rising $v_1 = 1$. Then the time is measured when respectively v_{100} and v_{500} reach the value 0.9, from which we can calculate the speed, c. We see in Figure 1 that the theory indeed

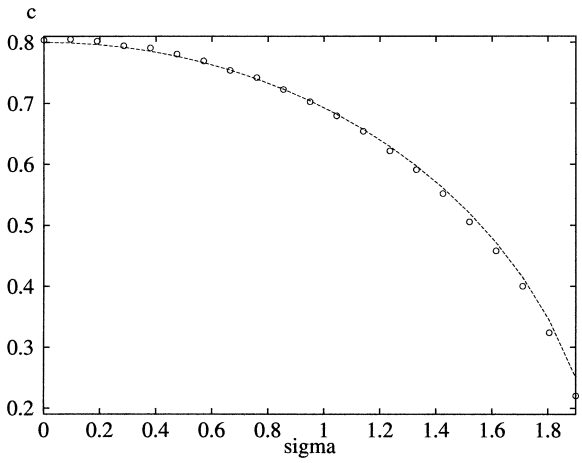

Figure 1. Comparison between theoretical propagation velocities (c_{th}, the curve) and the simulations (c, the circles) as a function of the "deviation", σ, for the Fisher equation with *periodic coupling* is shown. Here, $a = 0.1$ and $E(g) = 2$ so that $c_{\text{th}}^0 = 0.8$.

estimates the simulated speed very well, especially if the variance is not too big, and also get the right speed for the homogeneous case $\sigma = 0$, $c_{\text{th}}^0 = \frac{1-2\cdot 0.1}{\sqrt{2}}\sqrt{2} = 0.8$.

Varying $E(g)$ and a does not seem to change this conclusion as long as the parameters initiate a wave.

3.2. Randomly chosen coupling

Again we simulate a line of 500 cells modeled as given in the previous subsection. However, now the coupling strength is chosen randomly from a gamma-distribution *GAMMA*(a, b). The reasons for choosing the gamma-distribution (and not for example a normal distribution) are that we know the average of the inverse gamma-distribution, and will always have a positive coupling strength. We have for $X \sim$ *GAMMA*(a, b),

$$E(X) = ab, \quad \text{Var}(X) = ab^2, \tag{11}$$

and

$$\left(E\left(\frac{1}{X}\right)\right)^{-1} = (a-1)b = E(X) - \frac{\text{Var}(X)}{E(X)}. \tag{12}$$

So, also in this case we expect that the propagation velocity decreases with increasing variance following

$$c_{\text{th}}^{\text{Gamma}} = K\sqrt{E(X) - \frac{\sigma^2}{E(X)}}. \tag{13}$$

We hold $E(X) = 2$ constant as above, and vary $\sigma^2 = \text{Var}\,(X)$. Figure 2 shows that the theory predicts the simulated speed well.

The fit is not so good as in the periodic case because of the random factor. Comparing with the so-called *semi-theoretical* speed

$$c_{\text{semi}} = K\sqrt{\left(\frac{1}{400}\sum_{i=101}^{500}\frac{1}{g_i}\right)^{-1}}, \tag{14}$$

obtained from the actual coupling used in the simulation, we get a better fit. In this manner, we see that a large part of the difference between simulated and theoretical speeds arises from the random choice of coupling strengths rather than from a gap in the theory. Again, repeating the simulations does not change the conclusion, and of course, the average of many such simulation should fit the theoretical curve well.

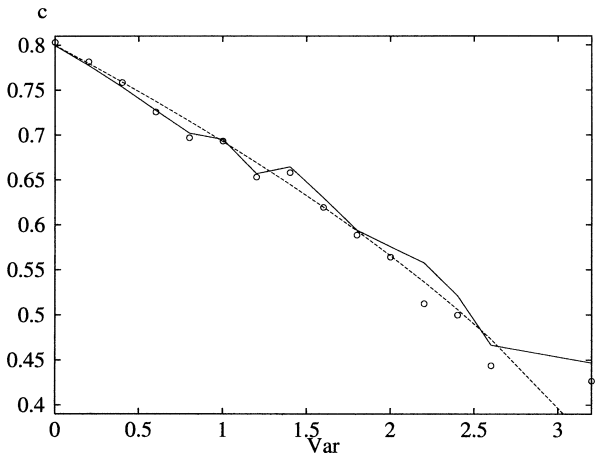

Figure 2. Comparison is shown between theoretical propagation velocities ($c_{\text{th}}^{\text{Gamma}}$, the punctuated, smooth curve), the semi-theoretical velocities (c_{semi}, the rugged curve) and the simulations (the circles) as a function of the variance, Var $= \sigma^2$, now for *Gamma-distributed* couplings. Again $c_{\text{th}}^0 = 0.8$. For Var > 2.6 most of these specific coupling strengths and initial conditions do not initiate a wave.

4. A Line of β-Cells

We simulate a line of β-cells using the same model as given in [1]. However, we choose the coupling strengths randomly, so that they vary along the line. This is in contrast to the simulations given in [1] where an identical coupling was assumed. We show how the propagation speed depends on the variance of the couplings. In particular, it is shown that the heterogeneity can provide another explanation why the simulations in [1] gave very high wave speeds.

4.1. Model and method

The model is taken from [9] and is given as follows with $j = 1,\ldots, 20$:

$$c_m \cdot \frac{dv_j}{dt} = I\left(v_j, n_j, s_j, Ca_j^i, Ca_j^{er}\right) + g_j(v_{j-1} - v_j) + g_{j+1}(v_{j+1} - v_j), \quad (15)$$

$$\frac{dn_j}{dt} = \frac{n_\infty(v_j) - n_j}{\tau_n}, \quad (16)$$

$$\frac{ds_j}{dt} = \frac{s_\infty(v_j) - s_j}{\tau_s}, \quad (17)$$

$$\frac{dCa_j^i}{dt} = f \cdot \left(\alpha I_{Ca}(v_j) - k_c Ca_j^i\right) + (J_{\text{out}} - J_{\text{in}}), \quad (18)$$

$$\frac{dCa_j^{er}}{dt} = \frac{J_{\text{in}} - J_{\text{out}}}{\rho}. \quad (19)$$

Here, v_j is the membrance potential, n_j and s_j are, respectively, fast and slow gating variables, Ca_j^i is the intra-cellular calcium concentration and Ca_j^{er} is the calcium concentration in the ER calcium stores for the j'th cell. The j'th cell is coupled through gap junctions to the neighboring cells $j-1$ with conductance g_j and $(j+1)$ with conductance g_{j+1}. The function I is the total membrance current, and I_{Ca} is one of these currents, a voltage-dependent calcium current. J_{in} and J_{out} are the currents going in and coming out of the ER stores, c_m is the total membrance capacity, n_∞ and s_∞ are steady states depending on v, τ_n and τ_s are time constants and f, α, k_c and ρ are constants. We impose the no-flux boundary condition, $v_0 = v_1, v_{21} = v_{20}$. For details see [9, 1] or Appendix for detailed expressions and parameter values.

The relation to Eq. (1) is given as follows (see also [1]). On the wave front we can uncouple the variables Ca^i and Ca^{er}, assuming that s is constant while $n = n_\infty(v)$ leaves only

$$c_m \cdot \frac{dv_j}{dt} = I(v_j, n_\infty(v_j); s) + g_j(v_{j-1} - v_j) + g_{j+1}(v_{j+1} - v_j),$$

of the same form as (1).

Simulations now result in similar conclusions as seen for the Fisher equation in Section 3: As the variance increases, the wave speed decreases.

Imposing a random initial condition on v_j results in a wave pattern after a very short transient period. The speed is found as the length between the center of the first and the last cell, $L = 20 \times 10\ \mu$m, divided by the (absolute) difference of the times when v_1, respectively, v_{20} increases through -60 mV signifying the beginning of an active period. Hence we count waves starting from either side of the line. To ensure that we do not count "false" beginnings we require that s_1, s_{20}, is less than 0.45 at the same time. This value was found empirically.

Now we take the average speed of many successive waves (until $t = 1000$ s), but only counting speeds between 30 and 500 μm/s (the typical simulated value is 100–250 μm/s, in experiments it is 30–100 μm/s). Hence, we rule out very fast waves because these are probably waves starting almost simultaneously from both sides, and very slow speeds because these are probably coming from errors in the measure method. For example, one could imagine that for a brief moment v_1 passes above -60 mV without starting a wave. However, the time is recorded, so when v_{20} increases above -60 mV much later, we will obtain a very small number for the speed. Such phenomena should of course be ruled out.

4.2. SIMULATIONS

Simulations of periodic coupling with $g_i = 100\ \text{pS} + (-1)^i \cdot \sigma$ as given in Section 3.1 are shown in Figure 3, where the simulated average wave speed is

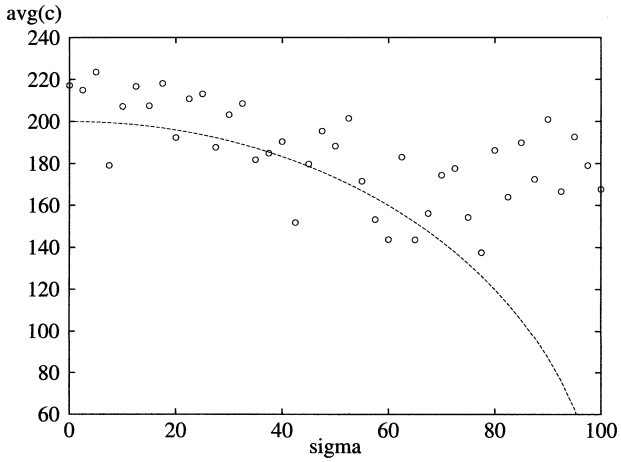

Figure 3. Comparison is shown between theoretical propagation velocities (c_{th}, the curve) and the simulations (the circles) as a function of the "variance," σ, for the β-cell model with periodic coupling, $g_i = 100\ \text{pS} + (-1)^i\sigma$.

compared with the theoretically expected value

$$c_{\text{th}} = 200\ \mu\text{m/s}\sqrt{1 - \left(\frac{\sigma}{100\ \text{pS}}\right)^2},$$

where 100 pS is the average coupling strength, and the value of 200 μm/s is chosen for obtaining a reasonable fit. This speed coincides with the speed found in [1]. We see that for σ below approximately 70 pS, the simulated and the theoretical values coincide pretty well, although there are large deviations. We claim, that at least the tendency seems to be, that for larger σ the wave is slower.

We repeat the simulation, but now with coupling strengths randomly chosen from a uniform distribution on $(\mu - d, \mu + d)$, i.e. coming from a stochastic variable $X \sim UNIF(\mu - d, \mu + d)$. The simulated wave speeds should be compared with

$$c_{\text{th}} = K\sqrt{E(1/X)^{-1}} = K\sqrt{\frac{2d}{\ln\left(\frac{\mu+\text{d}}{\mu-\text{d}}\right)1\text{pS}}}. \tag{20}$$

To distinguish whether the differences between the simulated speed and the speed coming from the limit equation is due to the actual chosen coupling strengths, we also compare with the semitheoretical value

$$c_{\text{semi}} = K\sqrt{\left(\frac{1}{19}\sum_{i=2}^{20}\frac{1\ \text{pS}}{g_i}\right)}. \tag{21}$$

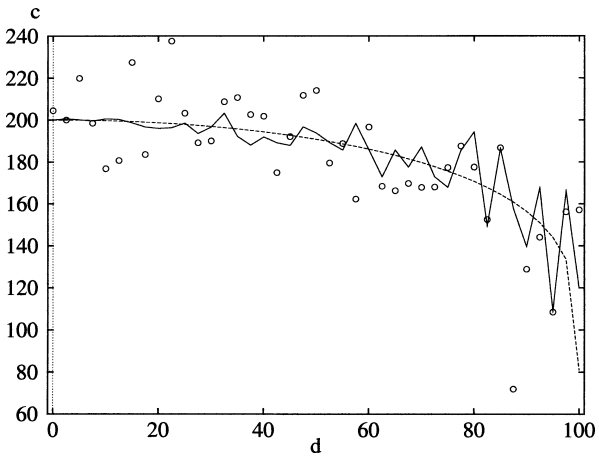

Figure 4. Comparison is shown between theoretical propagation velocities (c_{th}, the punctuated, smooth curve), the semi-theoretical velocities (c_{semi}, the rugged curve) and the simulations (the circles) as a function of d for the β-cell model with uniformly, randomly chosen coupling, *UNIF*(100 pS $-d$, 100 pS $+ d$). We know that the relation between d and the variance is Var $= \frac{d^2}{3}$. Here $K = 20$ μm/s, corresponding to a homogeneous velocity of 200 μm/s, is chosen to obtain a good fit.

Again, we hold $\mu = 100$ pS as fixed and vary d. Figure 4 shows that the simulated values are predicted well by the theoretical and the semitheoretical speeds, c_{th} and c_{semi}. Also, we see that these two values coincides well, and hence the simulated speeds are not different from the theoretical values because of a wrong predicted value for the relevant $(E(1/X))^{-1}$. This corresponds to the fact that we have discrepancies between the simulated and predicted speed even in the perfect periodic case.

By using the gamma-distribution the same conclusion is yielded as shown in Figure 5. Again we get a reasonable fit with the expected theoretical wave speed from Eq. (13), at least for Var < 8000 (pS)^2, or even better also for higher values of Var by using the semitheoretical values from Eq. (21).

The simulations with a normal distribution confirm the general picture, as shown in Figure 6. In this case we do not have a simple theoretical expression to compare the speed with. Instead, after many simulations, we found that the average decreases approximately from 210 μm/s to 150 μm/s. Because the normal distribution can result in negative values, we take special care in setting these couplings to 0, signifying no connection between the two cells (indicated with a dot in Figure 6). This should of course prohibit wave propagation. However, because the cells are self-excitory, we can get two independent waves on each side of the point without connection so that the overall picture could imitate a true wave. These cases should be ruled out which results in a slightly greater average speed (the speeds quoted above) than if these cases were included.

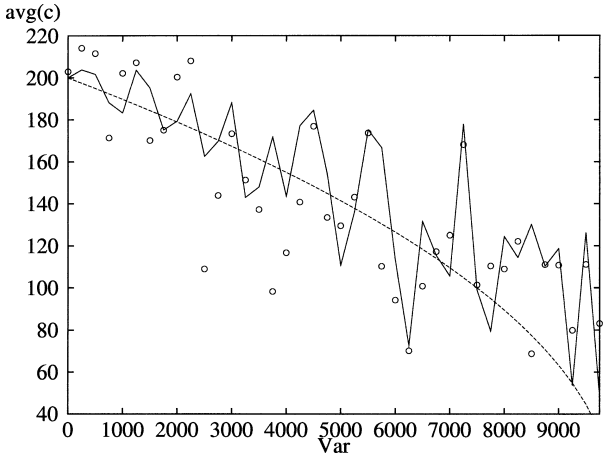

Figure 5. Comparison is shown between theoretical propagation velocities (c_{th}, the punctuated, smooth curve), the semi-theoretical velocities (c_{semi} the rugged curve) and the simulations (the circles) as a function of the variance, Var, for the β-cell model with randomly chosen coupling from a Gamma-distribution, $GAMMA(a, b)$ with $a = \frac{\mu^2}{\text{Var}}$, $b = \frac{\text{Var}}{\mu}$, where $\mu = 100$ pS is the average. Again we use the value 200 μm/s for the homogeneous case.

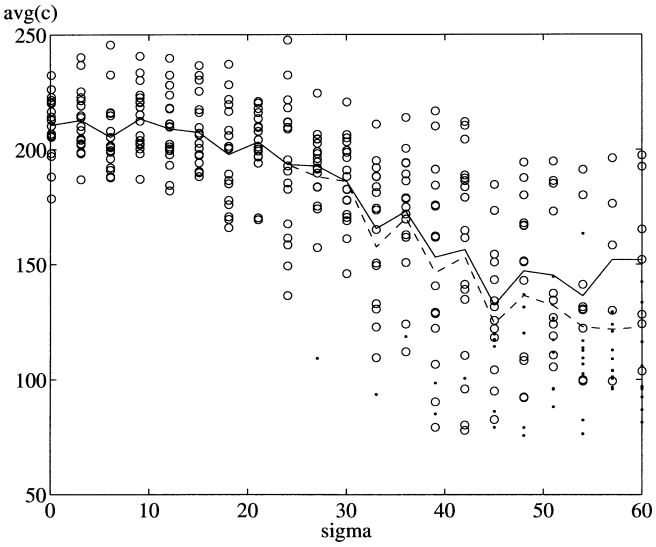

Figure 6. Several simulations were done of the wave speed for the line of β-cells with couplings chosen from a normal distribution $N(100 \text{ pS}, \sigma^2)$. For each choice of σ we did 18 simulations applying different configurations of the couplings. The circle indicates a simulation where all the couplings were positive, the dot indicates a simulation where one or more of the couplings were zero so that the line was not connected. The solid line indicates the average for the connected lines (the circles), the dashed line the average of all the simulations (the circles as well as the dots).

Note that we get average speeds as low as 80 μm/s for sufficiently large Var $= \sigma^2$ in all three cases. This is in the experimental range of (30–100 μm/s), hence we observe, as previously mentioned, another possible explanation for the fact that Aslanidi *et al.* found too large wave speeds in [1]—they did not consider the natural variance between the coupling strengths in an islet.

5. The Two-Dimensional Case

We have successfully simulated two-dimensional wave propagation. We considered a square lattice of 13 by 13 cells, each cell coupled to four nearest neighbors (N, S, E and W) with a no-flux boundary condition.

Using the Fisher equation and choosing random couplings, leads to similar conclusions as obtained in the one-dimensional case – for greater heterogeneity we find lower propagation speed, as shown in Figure 7. The speed was found over the center cells to rule out (part of) boundary phenomena and the fact that we start the wave in a corner, which influences the speed measured over the first few cells. In this case the speed is slightly higher than in the one-dimensional case (0.98 instead of 0.8 for $\sigma = 0$). We expect that this stems from boundary phenomena.

For the β-cell model, we used the simpler (v, n, s)-system from Eqs. (15)–(17), following Sherman [9]. We imposed heterogeneity by choosing the g_j's from a normal distribution $N(100 \text{ pS}, \sigma^2)$. Examples of two waves from our simulations are shown in Figure 8.

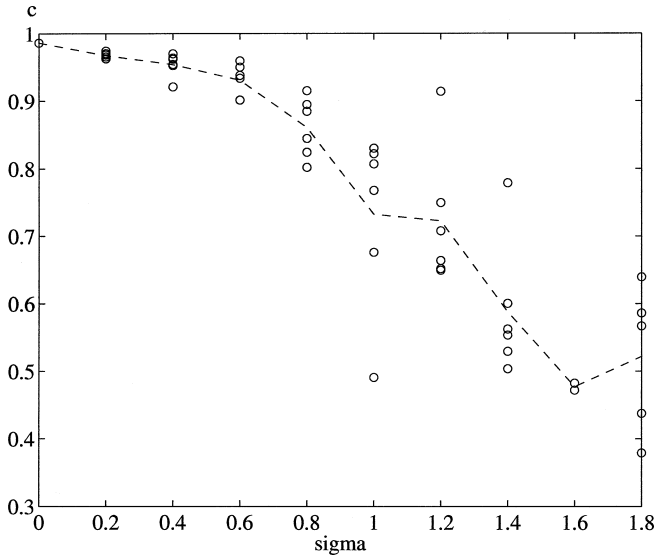

Figure 7. Six simulations for each choice of σ, of the two-dimensional Fisher equation with coupling strengths chosen from a normal distribution $N(2, \sigma^2)$, showing the speed as a function of the standard deviation σ. The curve shows the average speed of these six simulations.

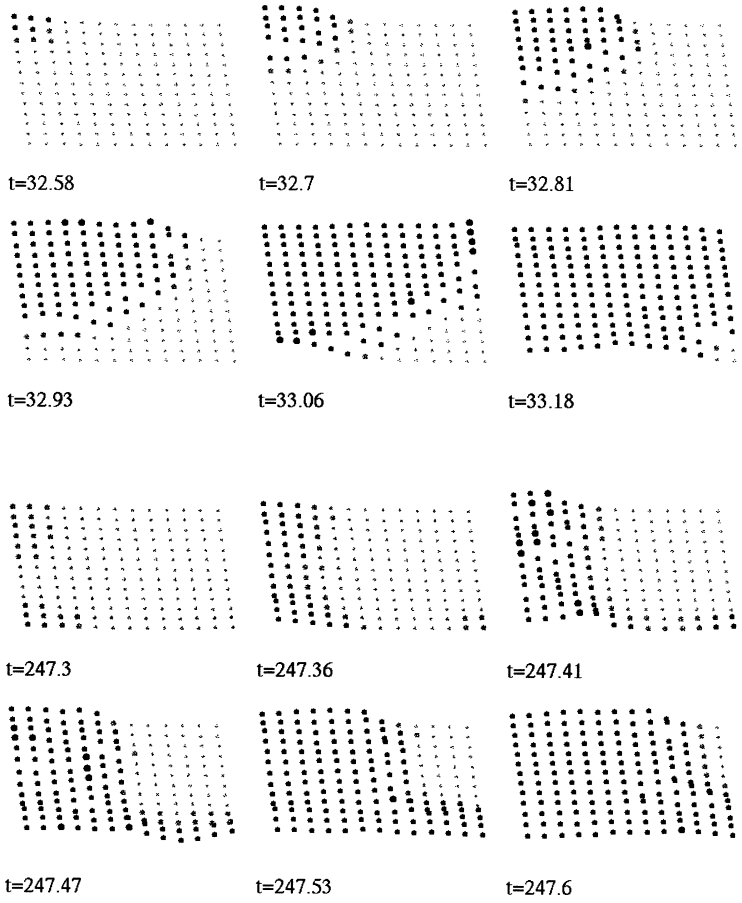

Figure 8. Two typical two-dimensional waves obtained from the (v, n, s)-subsystem of the β-cell model. In this simulation the coupling is chosen from a normal distribution, $N(100\text{ pS}, (53\text{ pS})^2)$. The upper figures show the most typical case, where the wave starts from just one corner. The lower ones show the case where the wave starts almost simultaneously from two corners (SW, NW), with a third (SE) starting "independently" slightly later. This results in a much higher measured wave speed.

The speed was found by requiring that all four corner cells should enter the active phase. The time from when this happened to the first, to the time it happened to the last of these cells, was recorded and the diameter of the "islet", $L = 12\sqrt{2} \times 10\ \mu\text{m} = 170\ \mu\text{m}$, was used as the distance the wave had traveled. In the two-dimensional case we do not rule out those cases where one or more of the g_j's have negative value; instead, we used the value 0, which implies that the two involved cells are not coupled. This indeed is the case for about 33% of cell pairs in an islet [7], but the wave can still propagate, using other couplings.

Again varying $\text{Var} = \sigma^2$ seems to have the same effect as seen in the one-dimensional case–for larger σ, the propagation velocity is lower, as shown in

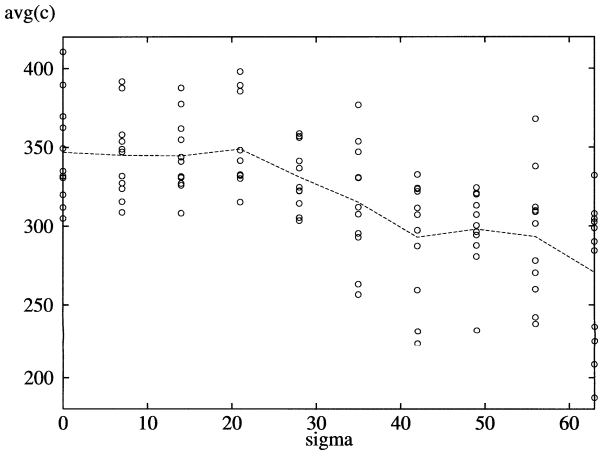

Figure 9. Propagation speeds from the (v, n, s)-subsystem of the β-cell model with coupling chosen from a $N(100, \sigma^2)$-distribution. For each choice of σ we did 11 simulations applying different configurations of the couplings. The circles indicate each such simulation and the curve shows the average of these 11 simulations, which decreased from 347 μm/s to 270 μm/s almost monotonously over the range from $\sigma = 0$ pS to $\sigma = 63$ pS.

Figure 9. Note that the wave speed is significantly greater, about 1.5–2 times as great as in the one-dimensional case.

6. Discussion

The main outcome of this paper is the fact that heterogeneity plays an important role in determining the wave speed of an excitation wave. In natural systems such as the islet of Langerhans, the cells are always coupled in a heterogenous manner. So far models have applied the average coupling strength found in experiments as a prototype coupling strength and then, assumed that the coupling was homogenous.

Here we have shown that for estimating the propagation velocity the variance of the coupling strengths plays a crucial role, both in the (pure mathematical) Fisher equation (Figures 1, 2 and 7) and in a standard model for the β-cells in an islet of Langerhans (Figures 3–6 and 9), for both the case periodic case (Figures 1 and 3) and the random case (Figures 2, 4–7 and 9), and further, both in the one- and two-dimensional cases. To the best of our knowledge, this is the first published literature on simulations of two-dimensional waves in a lattice model of an islet of Langerhans.

The dependence of the coupling on the variance was explained theoretically using the homogenization theory, which gave theoretic predictions of the propagation velocities using harmonic mean $(E(1/g))^{-1}$ instead of the average (arithmetic mean) $E(g)$. This theoretic result coincided well with the simulated speeds, especially when we took into account the deviations arising from the random choices

of coupling strengths using the semitheoretical speed. We believe that the use of the homogenization theory in modeling the β-cells is a new application. It has been used for a model of the cardiac tissue in [4]. However, from a different perspective, investigating propagation failure and the case of varying gap junctions is not considered explicitly. The heterogeneity there stems from the difference between the resistance in the cells and the resistance of the gap junctions.

However, we obtained excellent fits which simulated the theoretical results only for the Fisher equation. For the β-cell model the difference between the predicted and simulated velocities was greater. We suggest several possible explanations.

The first explanation could be that we used 500 "cells" for the simulation of the Fisher equation whereas only 20 cells were used for the β-cell model. Hence, we are closer to the continuum limit of $\epsilon \to 0$ given in the homogenization theory. In Figure 10, we see a simulation of the Fisher equation for 20 cells, and observe that the fit is still decent when we calculate the speed over the center cells (between cell numbers 8 and 12). The deviation for low variance seems to stem from boundary phenomena; when we calculated the speed over all the cells the deviation was found to be significantly greater. Similar boundary phenomena were found in the case of 500 cells, if we calculated the speed over the last 20 cells. Hence, this boundary phenomenon might explain some of the deviation for the β-cell, but the low number of cells do not matter directly if we take their boundaries into the account. This also explains why we found higher speeds from in the 2D-case (since the boundary is much larger here).

However, even for the periodic case of the β-cell in Figure 3, we did not obtain regular results. The boundary phenomena result in a nice pattern for the Fisher equation, and hence the same should be expected for the full β-cell model. The

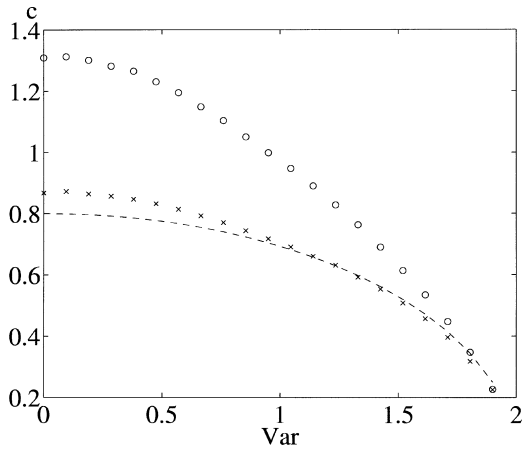

Figure 10. Simulated speeds from the Fisher equation, similar to Figure 1, but for 20 cells. The circles are simulated speed calculated as the speed over all the cells whereas the crosses are speeds (of the same waves) calculated over the center cells. The punctuated curve is obtained from the theoretical curve by using the theoretical result $c_{\text{th}}^0 = 0.8$.

β-cell model is known to admit chaos, even for a single cell [6], and the complex situation with 20 or more coupled cells should be expected to behave irregularly. The above fact complicates the calculation of the simulated wave speeds. The method chosen to find the speed in the simulations could indeed be doubted. We have done control simulations, going through the simulation in detail, and it seems that, in general, the automatic method described in Section 4.1 obtain the same result as a detailed "hands-on" calculation.

The simulations of the one-dimensional β-cell model showed that heterogeneity alone was sufficient to obtain velocities in the experimental region, and we claim that the fact that Aslanidi *et al.* in [1] used a homogenous coupling can explain the major reason why they obtained too high speeds.

Interestingly, in the case of a normal distribution, which is probably the most "natural" for a physical islet, these low velocities happen around the standard deviation $\sigma = 50$, i.e., for σ about half of the mean. Perez-Armendariz *et al.* [7] found experimentally that 67% of cell pairs were coupled with $g_j = 215 \pm 110$ pS, i.e., the standard deviation was about half of the average value. This might be an optimal ratio for proper islet functioning. If the variance is less, the waves are very fast, and if the variance is higher, too many cells will be uncoupled leading to insufficient synchronization. A low variance and/or fast waves could result in a lower responsiveness of the islet on glucose stimulation, as seen in experiments with gene-manipulated cell in the islet expressing abnormally strong connections [3]. The idea is that all the cells in the islets responded even to low glucose stimulations whereas in a normal islet only parts of the islet respond at low glucose levels, and that more cells are entrained for greater glucose stimulation. Naturally, a variating coupling strength would help in having such a behavior.

However, our two-dimensional simulations raised a new question: why do we obtain very high wave speeds in the 2D case but not in the 1D case? Indeed the experiments in [1] and elsewhere were practically two-dimensional, and hence the 2D case is of greater interest.

The fact that the wave is more likely to start independently at two corners (see Figure 8, lower part), so that it has to travel a shorter distance, can explain this. However, for the simulation shown in Figure 8 only 1 out of 15 waves started from two (or more) corners, and in none of the cases where the wave started from one corner did we find wave speeds less than 200 μm/s.

We also did one-dimensional control simulation of the reduced (v, n, s)-system, which gave results similar to the full system, that ruled out the possibility that the (Ca^i, Ca^{er})-variables are important.

As mentioned above boundary phenomena, which are more important in two dimensions because more cells are near the boundary, seem to be a plausible explanation. Indeed, we see in Figure 10 that the boundary phenomena can explain a rise of the wave speed of up to 50%, similar to the increased speed between one- and two-dimensional simulations for the β-cell model. If this is so, then there might be a property of the islet or some condition in the experiments might exist, so that

the no-flux boundary condition become inappropriate. Indeed, the center of an islet has a different structure than the parts near the surface ([5] and references therein). Or maybe, we simply require simulation of greater assemblies of cells—we did the simulations for $13^2 = 169$ cells. But in an islet there are of the order of 2000 cells, so if the cells were squished down to 2D with a height of e.g. three cells, we should simulate 26^2 cells, i.e., four times as many. Mads Peter Sørensen (personal communications) pointed out another possibility, which is that the curvature of the wave front might result in faster waves. We should pursue this possibility further. Finally, the 3D-case should be of interest—indeed $2000 \simeq 13^3$ so that the simulations presented here have a relevant size for this case.

In summary, the heterogeneity of the islet seems to have an important role in the control of insulin secretion in response to glucose stimulation. Here we have shown that the excitation waves spreading through the islet are modulated by the heterogeneity of the coupling strength, thereby suggesting a way of expressing the heterogeneity. Similar behavior should be expected in other organs consisting of heterogeneously coupled cells, or in ecology modeling having interactions on a smaller scale than that which is relevant for the full problem.

Acknowledgements

The author thanks "Rejselegat for Matematikere" (Travelling scholarship for Mathematicians) for financial support, "The Biomathematics Laboratory at IASI "A. Ruberti," CNR', Roma, Italy, for kindly letting me visit the Lab, where this work was carried out and Mads Peter Sørensen, IMM, Technical University of Denmark, for fruitful discussions.

Note

1. It seems reasonable to choose κ to be piece-wise constant if κ should model gap junctions, and this will be done in what follows. However, then κ is not differentiable so to justify the calculations leading to the PDE (3), we should use e.g. a smooth approximation of κ.

Appendix: The Equations and Parameters for The β-Cell Model

The functions and parameters of the Eqs. (15)–(19) are as follows:

$$\begin{aligned} I(v, n, s, Ca^i, Ca^{er}) &= I_s(v, s) + I_{\mathrm{Ca}}(v) + I_K(v, n) + I_{K,\mathrm{atp}}(v) \\ &\quad + I_{\mathrm{K,Ca}}(v, Ca^i) + I_{\mathrm{CRAC}}(v, Ca^{er}) \\ I_s(v, s) &= g_s \cdot s \cdot (v - v_k) \\ I_{\mathrm{Ca}}(v) &= g_{\mathrm{Ca}} \cdot m_\infty(v) \cdot (v - v_{\mathrm{Ca}}) \\ I_K(v, n) &= g_K \cdot n \cdot (v - v_k) \\ I_{K,\mathrm{atp}}(v) &= g_{K,\mathrm{atp}} \cdot (v - v_k) \end{aligned}$$

$$I_{K,\mathrm{Ca}}(v, Ca^i) = g_{K,\mathrm{Ca}} \cdot (v - v_k) \cdot \frac{(Ca^i)^5}{(Ca^i)^5 + k_d^5}$$

$$\begin{aligned}
I_{\mathrm{CRAC}}(v, Ca^{er}) &= g_{\mathrm{CRAC}} \cdot z_\infty(Ca^{er}) \cdot (v - v_{\mathrm{CRAC}}) \\
m_\infty(v) &= \frac{1}{(1 + \exp((v_m - v)/s_m))} \\
n_\infty(v) &= \frac{1}{1 + \exp((v_n - v)/s_n)} \\
s_\infty(v) &= \frac{1}{1 + \exp((v_s - v)/s_s)} \\
z_\infty(Ca^{er}) &= \frac{1}{1 + \exp((Ca^{er} - \bar{c}_{ER})/s_z)} \\
J_{\mathrm{in}}(Ca^i) &= \frac{v_p}{\mu} \cdot \frac{(Ca^i)^2}{(Ca^i)^2 + k_p^2} \\
J_{\mathrm{out}}(Ca^i, Ca^{er}) &= \frac{p_1}{\mu}(Ca^{er} - Ca^i)
\end{aligned}$$

The parameters used through out the work are:

$$\begin{aligned}
&g_{\mathrm{Ca}} = 1000 \text{ pS}, g_K = 2700 \text{ pS}, g_s = 200 \text{ pS}, g_{K,\mathrm{atp}} = 120 \text{ pS}, \\
&g_{K,\mathrm{Ca}} = 1000 \text{ pS}, g_{\mathrm{CRAC}} = 40 \text{ pS}, \\
&v_{\mathrm{Ca}} = 25 \text{ mV}, v_k = -75 \text{ mV}, v_m = -20 \text{ mV}, v_n = -16 \text{ mV}, v_s = -52 \text{ mV}, \\
&v_{\mathrm{CRAC}} = -30 \text{ mV}, s_m = 12 \text{ mV}, s_n = 5.6 \text{ mV}, s_s = 5 \text{ mV}, \\
&c_m = 5300 \text{ fF}, \tau_n = 20 \text{ ms}, \tau_s = 20000 \text{ ms}, \mu = 250 \text{ ms}, \\
&f = 0.01, k_c = 0.2 \text{ ms}^{-1}, \alpha = -4.5 \cdot 10^{-6} \mu\text{M}/(f A \cdot \text{ms},) \\
&k_d = 0.6,\ k_p = 0.1\ \mu\text{M}, v_p = 0.24\ \mu\text{M}, \bar{c}_{ER} = 4\ \mu\text{M}, s_z = 1\ \mu\text{M}, \rho = 5, p_1 = 0.02.
\end{aligned}$$

The diameter of a β-cell was set at 10 μm.

In the two-dimensional simulations we uncoupled (Ca^i, Ca^{er}) by neglecting $I_{K,\mathrm{Ca}}$ and I_{CRAC}. All parameters were left unchanged.

All simulations were done using the banded version of the CVODE solver of the program XPPAUT with standard tolerances.

References

1. Aslanidi, O.V., Mornev, O.A., Skyggebjerg, O., Arkhammar, P., Thastrup, O., Sørensen, M.P., Christiansen, P.L., Conradsen, K. and Scott, A.C.: Excitation Wave Propagation as a Possible Mechanism for Signal Transmission in Pancreatic Islets of Langerhans, *Biophys. J.* **80** (2001), 1195–1209.
2. Bensoussan, A., Lions, J.L. and Papanicolaou, G.C.: *Asymptotic Analysis for Periodic Structures*, North Holland, New York, 1978.
3. Charollais, A., Gjinovci, A., Huarte, J., Bauquis, J., Nadal, A., Martín, F., Andreu, E., Sánchez-Andrés, J.V., Calabrese, A., Bosco, D., Soria, B., Wollheim, C.B., Herrera, P.L. and Meda, P.:

Junctional Communication of Pancreatic β Cells Contributes to the Control of Insulin Secretion and Glucose Tolerance, *J. Clin. Invest.* **106** (2000), 235–243.
4. Keener, J.P.: 'Homogenization and Propagation in the Bistable Equation', *Physica D* **136** (2000), 1–17.
5. Mears, D., Sheppard, N., Atwater, I. and Rojas, E.: 'Magnitude and Modulation of Pancreatic β-Cell Gap Junction Electrical Conductance *In Situ'*, *J. Membr. Biol.* **146** (1995), 163–176.
6. Mosekilde, E., Maistrenko, Y. and Postnov, D.: *Chaotic Synchronization—Applications to Living Systems,* World Scientific, Singapore, 2002.
7. Perez-Armendariz, M., Roy, C., Spray, D.C. and Bennett, M.V.: Biophysical Properties of Gap Junctions Between Freshly Dispersed Pairs of Mouse Pancreatic Beta Cells, *Biophys. J.* **59** 1991, 76–92.
8. Scott, A.C.: *Nonlinear Science: Emergence and Dynamics of Coherent Structures,* Oxford University Press, Oxford, 1999.
9. Sherman, A.: Calcium and membrane potential oscillations in pancreatic β-cells in H.G. Othmer, F.R. Adler, M.A. Lewis and J.C. Dallon (eds.) *Case Studies in Mathematical Modeling: Ecology, Physiology, and Cell Biology,* Prentice-Hall, New York, 1997, pp. 199–217.